# The DNA methyltransferase inhibitor, guadecitabine, targets tumor-induced myelopoiesis and recovers T cell activity to slow tumor growth in combination with adoptive immunotherapy in a mouse model of breast cancer

**Andrea J Luker**
Virginia Commonwealth University https://orcid.org/0000-0003-3131-8049
**Laura J Graham**
Virginia Commonwealth University
**Matthew P Zellner**
Virginia Commonwealth University
**Jamie-Jean S Gilmer**
Virginia Commonwealth University Medical Center
**Sheela R Damle**
Virginia Commonwealth University
**Daniel H Conrad**
Virginia Commonwealth University
**Rebecca K Martin**
Virginia Commonwealth University
**Harry D Bear** ( harry.bear@vcuhealth.org )
https://orcid.org/0000-0002-7632-9019

**Research article**

**Keywords:** Myeloid Derived Suppressor Cells, DNA Methyltransferase Inhibitor, Immunotherapy, T lymphocytes, Myelopoiesis

**Posted Date:** October 10th, 2019

**DOI:** https://doi.org/10.21203/rs.2.15818/v1

**Version of Record:** A version of this preprint was published on February 27th, 2020. See the published version at https://doi.org/10.1186/s12865-020-0337-5.

# Abstract

Background: Myeloid derived suppressor cells (MDSC) represent a significant hurdle to cancer immunotherapy because they dampen anti-tumor cytotoxic T cell responses. Previous groups, including our own, have reported on the myelo-depletive effects of certain chemotherapy agents. We have shown previously that decitabine increased tumor cell Class I and tumor antigen expression, increased ability of tumor cells to stimulate T lymphocytes, depleted tumor-induced MDSC in vivo and augmented immunotherapy of a murine mammary carcinoma.

Results: In this study, we expand upon this observation by testing a next-generation DNA methyltransferase inhibitor (DNMTi), guadecitabine, which has increased stability in the circulation. Using the 4T1 murine mammary carcinoma model, in BALB/cJ female mice, we found that guadecitabine significantly reduces tumor burden in a T cell-dependent manner by preventing excessive myeloid proliferation and systemic accumulation of MDSC. The remaining MDSC were shifted to an antigen-presenting phenotype. Building upon our previous publication, we show that guadecitabine enhances the therapeutic effect of adoptively transferred antigen-experienced lymphocytes to diminish tumor growth and improve overall survival. We also show guadecitabine's versatility with similar tumor reduction and augmentation of immunotherapy in the C57BL/6J E0771 murine breast cancer model.

Conclusions: Guadecitabine depleted and altered MDSC, inhibited growth of two different murine mammary carcinomas in vivo, and augmented immunotherapeutic efficacy. Based on these findings, we believe the immune-modulatory effects of guadecitabine can help rescue anti-tumor immune response and contribute to the overall effectiveness of current cancer immunotherapies.


# Background

Tumors avoid immune detection and attack through a variety of mechanisms that circumvent the anti-tumor response. DNA hypermethylation, though reversible, can silence the expression of immunogenic antigens; this makes the immune system less effective, especially during immunotherapeutic interventions(1). Tumors also recruit regulatory immune cells, including MDSCs, which dampen the adaptive immune response. Patients with higher levels of circulating MDSCs have increased primary tumor growth(2), higher metastatic burden(3), more advanced clinical cancer stage(4,5), and shorter overall survival(3,6). Based on these findings and multiple reports in mouse models that implicate MDSCs as key obstacles to successful cancer immunotherapy, there has been much interest in eliminating the suppressive nature of MDSCs to improve patient outcomes(7–10).

Our lab has previously published on the effects of the DNA methyltransferase inhibitor (DNMTi), decitabine. Using the aggressive murine breast cancer line, 4T1, we found that decitabine improved the immunogenicity of these cells *in vitro,* and augmented the effects of adoptive immunotherapy (AIT) *in vivo(*10). While decitabine caused a reduction in tumor-induced MDSC accumulation, the underlying mechanism behind this was never investigated. In our current study, we have expanded upon these

findings with the second-generation DNTMi, guadecitabine, and investigated its mechanism of action in tumor reduction. Like the active metabolite decitabine, we found that guadecitabine diminished tumor-induced granulocytosis in 4T1 tumor-bearing mice. As a result of the reduced MDSC accumulation, guadecitabine rescued immune activation and was able to reduce tumor growth in a T cell-dependent manner. Guadecitabine was similarly effective in an E0771 model of murine breast carcinoma. Finally, we found that guadecitabine in combination with AIT resulted in prolonged survival in both 4T1 and E0771 breast cancer models. Because of these advantageous effects, guadecitabine could prove to be a beneficial new drug to reduce systemic immune suppression and augment the effectiveness of immunotherapy in cancer patients.

# Results

*Guadecitabine treatment in vivo reduces tumor size and specifically targets the myeloid lineage with minimal effects on lymphoid populations*

4T1 tumor-bearing WT Balb/cJ mice were treated daily on days 10, 11, 12, and 13 with 50g guadecitabine. By day 16, guadecitabine treatment had resulted in a significant reduction in tumor volume (*Figure 1a).*. Histologic examination revealed that control tumors had thick outer capsules surrounding the majority of the tumor, while tumors from guadecitabine-treated mice had thinner capsules that were often disrupted or fragmented. Tumors from guadecitabine-treated mice also had a higher prevalence of $TUNEL^+$ apoptotic cells (*Figure 1b).*

Progression of certain cancers can force the bone marrow and spleen into a phase of excessive myelopoiesis, whereby immature myeloid cells spill out into circulation. This accumulation of myeloid cells is the underlying cause of the splenomegaly seen in the 4T1 model, and provides a reservoir of recirculating MDSCs(7,11,12). Indeed, within the spleens of control 4T1 tumor-bearing mice we saw a large increase in cellularity due to a massive expansion of total MDSCs (*Figure 1c),*, with the granulocytic MDSCs accounting for 27.75% ± 1.627% of the total cell population (*Supplemental Figure 1a).*. There was a similar increase in total cellularity and number of MDSCs found in the bone marrow and blood (*Figure 1d,e),*, as has been previously reported(12–14). Representative flow images for each treatment group and tissue sample are shown in *Supplemental Figure 2.* With guadecitabine treatment, however, the excessive myeloid populations were largely absent in each tissue compartment. In the remaining splenic MDSCs, we saw a significant increase in the immune-stimulatory markers MHC II, CD80, and CD86 (*Figure 1f).*. Together, these data suggest that guadecitabine depletes MDSCs by targeting excessive myelopoiesis. Additionally, guadecitabine appears to push remaining MDSCs toward a mature, APC phenotype.

While reducing suppressive myeloid cells can be beneficial, the lymphoid compartment is vital for anti-tumor immunity. Because of the robust MDSC expansion in the spleen, the percentage of B and T cells at day 16 was reduced in control tumor-bearing mice (*Supplemental Figure 1b,c).*. The absolute number of B and T cells was increased, suggesting immune activation. In guadecitabine-treated mice, the B and T cells were present at normal, although not elevated above, naïve levels. Additionally, the highly ordered

structure of the spleen is essential to ensure proper cellular interactions. H&E staining illustrates that tumor-bearing control spleens have an enlargement of the red pulp due to accumulated MDSCs *(Supplemental Figure 1d).* This expansion is absent with guadecitabine treatment, and importantly the spleens maintain appropriate separation of red and white pulp. Based on the cell numbers and intact architecture, guadecitabine does not appear to affect the splenic lymphoid populations.

To investigate the temporal effects of guadecitabine, we next performed a time-course study. We observed an immediate slowing of tumor growth that reached significance by day 16 (*Figure 2a). Figure 2b-d* shows a steady increase in spleen, bone marrow, and blood cellularity from control tumor-bearing mice. MDSCs begin to accumulate in the bone marrow and blood around day 12, while the splenomegaly was slightly delayed until day 14. In each of these tissue compartments, however, guadecitabine instantly halted and reversed the accumulation of MDSCs. By day 16, the total MDSC populations were back to naïve levels.

*Guadecitabine's effect on tumor growth is T cell-dependent*

CTLs are the main effector cells responsible for cell-mediated killing of tumors. During an adaptive immune response, antigen-specific T cells become activated and expand to boost their anti-tumor activity. MDSCs have been shown many times to diminish the cytotoxic ability of CTLs in tumor-bearing hosts(7,8,15–21). We therefore wanted to investigate whether the reduced tumor burden resulted from a direct effect of guadecitabine on the 4T1 tumor cells *in vivo* or was secondary to the immunomodulatory effect of the drug.

Athymic nude mice bearing 4T1 tumors were either untreated or treated with guadecitabine as above. The tumors grew at an equal pace with or without guadecitabine (*Figure 3a,b).*. The treatments had the same effect of reversing the tumor-induced increase in cellularity and MDSC accumulation within the spleen, bone marrow, and circulation (*Figure 3c-e).*. TUNEL staining of the tumor, however, indicated no obvious apoptotic cells in either group (*Figure 3f),*, indicating that guadecitabine does not have a direct cytotoxic effect on 4T1 tumors. Together, these data suggest that the effect of guadecitabine on tumor growth is T cell-dependent.

In order to confirm the role of T cells, we performed a series of depletion experiments to target and remove T cells with depletion antibodies according to the schedule in *Supplemental Figure 3a.* We confirmed the specificity and completeness of the -CD4 and -CD8 depletions, showing that only the intended T cell populations were removed without affecting B cells and MDSCs (*Supplemental Figure 4).* As expected, mice receiving the isotype control + guadecitabine had smaller tumors than the isotype alone (*Supplemental Figure 3b).*. In mice which underwent $CD8^+$ T cell depletion, however, we observed comparable tumor growth with or without guadecitabine treatment (*Supplemental Figure 3c).*. When $CD4^+$, in addition to $CD8^+$, cells were depleted, there was no additional effect on the tumor, suggesting $CD4^+$ T cells do not play a significant role (*Supplemental Figure 3d).*. Together, these experiments confirm

the role of T cells, but also indicate that $CD8^+$ CTLs are the important population involved in the enhanced tumor immunity.

*Guadecitabine diminishes the T cell-inhibitory environment of the spleen*

The dLN is a site of robust immune activity and often of great interest in tumor studies(22). We harvested dLN from WT tumor-bearing control or guadecitabine-treated mice on day 16 and restimulated the cells *in vitro* with ionomycin+PMA. Flow cytometry analysis showed no difference in the percent of $CD8^+$ T cells producing IFN from guadecitabine-treated mice versus tumor-bearing controls (*Figure 4a).*. We did not observe MDSC infiltration into the dLN (*Supplemental Figure 5a)* of these mice, leading us to conclude that T cells are being affected elsewhere.

Several groups have published on the importance of the spleen as a priming zone for T cell activity(7,21). Others have previously reported on the requirement of direct contact between MDSCs and T cells in order for suppression to occur(19,21). We therefore hypothesized that the MDSC accumulation within the spleen interacts with and suppresses CTLs as they recirculate. When day 16 splenocytes were restimulated in culture, there was a significant increase in the percent of $CD8^+$ cells from guadecitabine-treated mice that produced IFN (*Figure 4b).*. To further investigate the T cell activity, we calculated the total number of IFN-producing $CD8^+$ T cells between the groups and found no difference (*Figure 4c).*. This reveals that guadecitabine elicits a higher degree of activation from the same number of splenic CTLs. This enhanced activation is further evidenced by the greater proportion of IFNγ-producing cells within the spleen (9.663% ± 0.9034) compared to the highly active dLN (5.149% ± 0.6741). We also confirmed previous reports that MDSCs only affect $CD8^+$ T cells(19), as we saw no effect on IFNγ production by $CD4^+$ T cells (*Supplemental Figure 5b).*.

*Used in combination with AIT, guadecitabine further slows tumor growth and prolongs overall survival*

We next tested the efficacy of guadecitabine administered in combination with the transfer of antigen-experienced lymphocytes. Lymphocytes from tumor-bearing donor mice were expanded *ex vivo* as previously described, resulting in 94.4% T cell purity (*Supplemental Figure 6)(*(10). Recipient animals were challenged with a 50,000-cell 4T1 flank tumor on day 0 then treated as shown in *Figure 5a.* Briefly, CYP and lymphocyte transfer coincided with the first treatments of guadecitabine on days 3 and 4. We observed a beneficial reduction in tumor size in mice that received guadecitabine or AIT alone. When combined, however, there was an impressive four-week delay in tumor growth, with complete regression in 2 of 5 mice (*Figure 5b)* and improved survival (*Figure 5e).*. Statistical significance was determined up to day 17, when all treatment groups remained experimentally viable. By comparing the areas under the curves (AUC), each treatment group was significantly reduced compared to the control mice(23). Additionally, the tumor measurements at day 17 show that the combination therapy resulted in significantly reduced tumor areas beyond guadecitabine or AIT alone. This separation of tumor growth curves continued to increase as the experiment progressed.

We also tested a different schedule, in which the CYP/AIT was delayed until the last treatment of guadecitabine on day 6 (*Supplemental Figure 7a);* this allowed time for guadecitabine to take effect before the antigen-experienced lymphocytes were introduced and poses a greater challenge to the efficacy of AIT against larger tumors. In this case, the synergistic effect of guadecitabine and AIT persisted further out until day 40 (*Supplemental Figure 7b).*. In addition, 4 of 5 mice were cured, and we observed a higher overall survival when AIT occurred after guadecitabine (*Supplemental Figure 7e)* with similar statistical significance (*Supplemental Figure 7c,d).*.

*Guadecitabine similarly reduces E0771 tumor burden.*

Finally, we wanted to test the effectiveness of guadecitabine in another breast cancer model. WT C57Bl/6 mice were injected subcutaneously with 200,000 E0771 cells. The tumors were allowed to become established for 3 days before the mice were treated daily on days 3, 4, 5, and 6 with 50g guadecitabine. Similar to the 4T1 model, guadecitabine significantly reduced the growth of E0771 tumors (*Figure 6a).*. Additionally adding guadecitabine significantly improved the impact of AIT (*Figure 6b,c).*.

# Discussion

There is great difficulty in treating neoplastic disease, especially when the tumor becomes resistant to chemotherapy. Today, the most promising interventions involve boosting the patient's own immune system to detect and destroy abnormal cells. Immunotherapy has emerged as a highly promising and effective treatment for a variety of cancer types, but still only a minority of patients exhibit strong objective responses. Tumors can employ several "tactics" to avoid recognition and suppress anti-tumor immune response. Through hypermethylation, tumors can silence immunogenic antigens to avoid cell-mediated killing. Additionally, the tumor environment can induce massive myelopoiesis, causing suppressive MDSCs to accumulate in the bone marrow, spleen, circulation, and in the tumor. For these reasons, there is great interest in finding ways to reverse these effects, thus allowing the immune system to clear the tumor.

Several groups have reported on the myelo-depleting properties of demethylating drugs such as decitabine(20,24) and 5-Azacitadine (AZA)(25), as well as other chemotherapy drugs, including gemcitabine(26,27), doxorubicin(8) and docetaxel(28). Although MDSCs are not being directly targeted, they seem to uptake the drugs more readily and are more susceptible to their effects. Guadecitabine, also known as SGI–110, was specifically designed to be resistant to degradation by cytidine deaminase and prolong the exposure of tumor cells to the active metabolite, decitabine. *In vivo,* guadecitabine treatments resulted in a near-complete absence of MDSCs in tumor-bearing mice (*Figure 1c-e).*. Based on the time-course experiment (*Figure 2),* it appears that guadecitabine treatment is *preventing,* rather than reversing, MDSC accumulation. We believe guadecitabine targets the bone marrow by diminishing the highly proliferative myeloid progenitors (*Figure 2c).*. This prevents increased MDSC circulation (*Figure 2d)* and accumulation within the spleen (*Figure 2b).*. Surprisingly, we found that the similarly proliferative 4T1 tumor cells were not vulnerable to cytotoxic effects of *in vivo* guadecitabine treatments (*Figure 3f).*.

Within the spleen of tumor-bearing mice we showed an accumulation of MDSCs in the red pulp (*Supplemental Figure 1d).*. This perilymphoid localization puts the MDSCs in contact with recirculating $CD8^+$ CTL. Several tumor studies have portrayed the spleen as an inhibitory environment that can diminish CTL function(7,29). In experiments by Ugel *et al,* the investigators removed the inhibitory MDSC environment through splenectomies(7). Although this did not affect tumor size, they found that T cell activation was recovered despite normal MDSC frequency within the blood and other tissues. This highlights the spleen's unique role as an isolated region of suppression with the ability to severely dampen the anti-tumor immune response. In the present study, we use guadecitabine to ablate the suppressive splenic environment. We found that IFN production within the dLN is comparable between WT and guadecitabine-treated mice (*Figure 4a).*. Upon recirculating through the spleen, however, WT CTLs have diminished activation (*Figure 4b)* even though the number of activated cells remained the same (*Figure 4c).*. This data supports the role of the spleen as an important suppressive zone that contributes to tumor progression.

Unlike Ugel's splenectomy experiments, our treatment additionally resulted in slower tumor growth (*Figure 2a),*, indicating guadecitabine may have a beneficial impact beyond the removal of regulatory myeloid populations. The enhanced tumor immunity may arise from guadecitabine's effect on MDSC phenotype. Although the majority of the MDSCs are eliminated, a small percentage of cells remained that are induced to express APC markers such as MHC II and CD80/86 (*Figure 1f).*. These data suggest that guadecitabine pushes suppressive MDSCs to develop into an immune-stimulatory phenotype to augment immune activation within the spleen.

The Ugel experiment also emphasizes a significant problem with a popular and promising clinical therapy. Animals that underwent sham surgeries responded poorly to AIT compared to those that received splenectomies. When the antigen-experienced T cells circulate through the suppressive spleen, they are inactivated despite being primed to target the tumor. Here we have shown a similar phenomenon; while AIT was effective in slowing the growth rate of the tumor, combination therapy with AIT+guadecitabine compounded this effect and resulted in persistent tumor suppression (*Figure 5b)* and prolonged survival (*Figure 5e).*. It is interesting to note that in the AIT experiments, guadecitabine was administered earlier at days 3, 4, 5, and 6 (*Figure 5),*, rather than days 10, 11, 12, and 13 (*Figures 1–4).*. This dosing schedule still resulted in slower tumor growth through day 16, although the reasons why are unclear. As we showed in *Figure 2b,* splenomegaly does not occur in our model until around day 14, correlating with the accumulation of MDSCs. We hypothesize that guadecitabine treatment targets the bone marrow, disrupting the abnormal myelopoiesis before it can begin. Further, we tested the effectiveness of delaying adoptive T cell transfer until the final guadecitabine treatment rather than being delivered concomitantly with the initial treatment (*Supplemental Figure 7).*. The delayed AIT alone was more effective at days 6 and 7 than at days 3 and 4, perhaps because the tumor has become more immunogenic and vascularized by the later date.

Finally, we showed the effectiveness of guadecitabine in slowing the growth of another tumor line on a different background strain. Although E0771 is not known to elicit a robust leukemoid reaction, studies

still indicate a suppressive role for MDSCs in this model(30,31). We observed a similar and persistent reduction in tumor growth with guadecitabine alone, or in combination with AIT.

# Conclusions

In conclusion, we have shown guadecitabine to be a multifaceted treatment against the aggressive 4T1 and E0771 breast cancer lines. Guadecitabine targets excessive myelopoiesis within the bone marrow and greatly reduces MDSCs within the spleen and blood. This eliminates the systemic suppression, thereby rescuing the host's anti-tumor CTL response. We've also shown guadecitabine significantly improves AIT treatment by providing an environment in which the transferred T cells can maintain their antigen-specific activity long-term. Because of the advantageous effects on multiple targets, guadecitabine could prove to be a beneficial new drug to reduce systemic immune suppression and augment the effectiveness of immunotherapy in cancer patients.

# Methods

*Animals*

Wildtype (WT) female Balb/cJ, C57Bl/6J, and athymic NU/J mice 8–10 weeks old were purchased from Jackson Laboratory. The health report was consistent with that of our Barrier Vivarium facility. Balb/cJ mice weighed an average of 20 grams prior to the start of experiments and C57Bl/6J mice weighed an average of 20 grams prior to the start of experiments. All mice were housed within Virginia Commonwealth University vivarium facilities, specifically the Massey Cancer Center Barrier Vivarium, in accordance with the humane treatment of laboratory animals set forth by the NIH and the American Association for the Accreditation of Laboratory Animal Care (AAALAC). All animal experiments were conducted with the permission and oversight of the Virginia Commonwealth University Institutional Animal Care and Use Committee (IACUC) under the protocols AM10065, and AM10256.

All animals were housed with 12 hour light and dark cycle in NexGen Cages from Allentown (194mm x 181mm x 398mm) on ventilated racks with corncob bedding (Shepard's Specialty Corn Cob Plus). The temperature maintained in the cages is between 68 to 76 degrees Fahrenheit. Five animals are housed per cage. Animals are fed Envigo Teklad 2919 and given water *ad libitum* via Lab Product's Hydropacs.

Animals were euthanized by isoflurane or $CO_2$ inhalation, followed by cervical dislocation.

*Experimental models and guadecitabine treatment*

50,000 4T1 or 200,000 E0771 cells in 50L PBS were injected subcutaneously into the flank at day 0. Cagemates were randomly assigned to differing groups at the start of the experiment. Appropriate groups received *i.p.* injections of 50g guadecitabine (kindly provided by Astex Pharmaceuticals, Inc.) on days 10, 11, 12, and 13, unless otherwise indicated. All injections took place between the hours of 10am to 2pm, working from the home cage. For each treatment, the control group was initially treated, followed by the

non-control groups. Mice were euthanized on day 16, when we collected blood by cardiac puncture, bone marrow from femurs and tibias, tumors, spleens, and inguinal lymph nodes.

T cell depletion was performed as previously described(32). Briefly, mice were injected *i.p.* with 200g of monoclonal antibodies on days 6, 7, 8, 9, and 14. Upon sacrifice, T cell depletion was confirmed in the spleen by flow cytometry. $CD4^+$ and $CD8^+$ T cells were depleted using the clones GK1.5 and 2.43, respectively (antibodies generated in house). Rat IgG was used as an isotype control.

AIT was performed as previously described(10). Briefly, donor Balb/cJ or C57Bl/6 mice were injected with $5x10^5$ 4T1 or E0771 cells, respectively, into the hind footpad; popliteal lymph nodes were collected at day 10 and activated overnight with bryostatin (5nM, Calbiochem) and ionomycin (1M, Calbiochem) in the presence of recombinant IL–2 (Peprotech). Cells were then washed and expanded in IL–7 and IL–15 (both 10 ng/mL, Peprotech) for one week. On the indicated day, tumor-bearing recipient mice were treated *i.p.* with 100mg/kg of cyclophosphamide (CYP). 24 hours later, 50 million expanded lymphocytes were infused intravenously. All groups, except control mice, received a single CYP treatment. Tumor areas were measured through the skin on live animals using digital calipers as length x width; tumor volumes represent length x width x height of excised tumors. Animals were observed at least three times per week, according to IACUC standards. Animals were euthanized upon reaching a humane endpoint, including tumor area >100$mm^2$, severe ulceration, or weight-loss.

*Organ processing and cell counts*

Blood volume collected by cardiac puncture was recorded and used to calculate the normalized number of cells per milliliter. Whole spleens were crushed to obtain a single cell suspension, then red blood cells were removed with ACK lysing buffer (Quality Biological). Femurs and tibias from each mouse were cleaned of connective tissue and spun at 350xg for 5 minutes to collect marrow before removing red blood cells. Viable cell counts were performed using trypan blue exclusions.

*Flow cytometry*

Single cell suspensions were obtained and stained with the fixable live/dead stain ZombieAqua (Biolegend) per manufacturer's instructions. Samples were then Fc-blocked with 2.4G2(33) for 5 minutes and stained for 30 minutes on ice. Flow samples that included multiple Brilliant Violet antibodies were stained in the presence of Brilliant Stain Buffer (BD Biosciences) per manufacturer's instructions. All cells were then fixed in 4% paraformalydehyde (PFA) fixation buffer (Biolegend) for 15 minutes at room temp. For intracellular staining, fixed cells were permeabilized with PermWash Buffer (Biolegend) per manufacturer's instructions. Flow data were collected using a BD LSRFortessa running BDFACSDiva™ 8.0 software, and analyzed with FlowJo (10.4.2). Total MDSCs were characterized as both monocytic and granulocytic populations combined. Gating for MDSC populations are as follows: $CD11b^+$ $Ly6C^{hi}$ (monocytic-MDSCs) and $CD11b^+$ $Ly6C^{int}Ly6G^+$ (granulocytic MDSCs). B cells were gated as MHC $II^+$ $B220^+$, and T cells were gated as $B220^-$ $CD4^+$ or $CD8^+$. The antibody clones were as follows: Ly6C (clone

HK1.4), Ly6G (1A8), IFN (CMG1.2), CD80 (16–10A1), CD86 (GL–1), I-A/I-E (M5/114.15.2), all from Biolegend, and CD45R/B220 (RA3–6B2), CD4 (GK1.5), CD11b (M1/70), all from BD Biosciences.

*Histology*

Some spleens and tumors were fixed with 4% PFA for 15 minutes then equilibrated with successive incubations in 10%, 20%, and 30% sucrose before being mounted in Optimal Cutting Temperature (OCT) medium. 10m cryo-sections were briefly fixed in ice-cold acetone then in 4% PFA prior to staining. Light microscopy slides were stained using ApopTag Plus Peroxidase In Situ Apoptosis Detection Kit (Millipore Sigma) followed by counterstaining with Meyer's Hematoxylin then imaged using an Olympus BX41.

*Cell lines*

4T1 (ATCC CRL–259) and E0771 cell lines were purchased from ATCC and CH3 Biosystems, respectively. Cell lines were maintained at low passage numbers and ATCC-recommended tests were performed, including morphology checks and mycoplasma screening.

*Ex vivo restimulation for IFN production*

All cells from each individual tumor-draining lymph node (dLN) or $10^6$ total splenocytes were plated in 2 mL media and restimulated with PMA (250ng/mL) and ionomycin (1M) in the presence of monensin and brefeldin A (Biolegend). After three hours, the cells were washed and permeabilized before being stained for intracellular IFN for flow cytometry.

*Statistics*

Each figure depicts one representative experiment of at least three independently conducted experiments. *n* values vary between 3–5 animals per group, per experiment. The number of experimental animals was determined based on data from spread in previous tumor experiments, while taking into account the need to reduce the use of unnecessary animals in research. For un-paired comparisons, a Student's t test was performed. Where appropriate, a one-way ANOVA with Tukey's or a two-way ANOVA with Sidak's multiple comparison tests was used when analyzing 3+ normally distributed data-sets (specific test indicated in legend). All statistical analyses were performed using GraphPad Prism 7. Significance is indicated in individual figure legends.

## Abbreviations

# AIT - Adoptive immunotherapy

# AUC - Area under the curve

# AZA5-Azacitadine

# CYP - Cyclophosphamide

# dLN - Draining lymph node

# DNMTiDNA - methyltransferase inhibitor

# OCT - Optimal cutting temperature

# PFA - Paraformaldehyde

# WT - Wildtype

## Declarations

*Ethics approval and consent to participate*

All animal experiments were conducted with the permission and oversight of the Virginia Commonwealth University Institutional Animal Care and Use Committee (IACUC) under the protocols AM10065, and AM10256

*Consent for publication*

N/A

*Availability of data and materials*

The datasets used and/or analysed during the current study available from the corresponding author on reasonable request.*Competing Interests*

The authors declare that they have no conflict of interest.

*Funding*

The study was funded by the NIH-National Institute of Allergy and Infectious Disease (NIAID) RO1AI8697A1 to RM (co-corresponding author) and a VCU Massey Cancer Center Pilot Project grant to

DC (co-author) and HB (co-corresponding author). The funding sources had no role in the study design, collection, analysis or interpretation of the data.

*Authors' contributions*

AL was responsible for substantial scientific and intellectual contributions to experimental design, data acquisition, including analysis, interpretation, and reporting of results. LG provided major contributions to data acquisition. MZ, and JG contributed to data acquisition and analysis. SD was responsible for the project conception and securing funding. RM contributed to data acquisition, analysis, editing of the manuscript, and critical feedback. DC and HB provided substantial scientific and intellectual contributions to the conception and evaluation of the project, editing of the manuscript and critical feedback. All authors have read and approved the manuscript.

*Acknowledgements*

Special thanks to Astex Pharmaceuticals, Inc. for kindly providing guadecitabine. Services and products in support of the research project were generated by the Virginia Commonwealth University (VCU) Massey Cancer Center Flow Cytometry Shared Resource. Microscopy was performed at the VCU Microscopy Facility. Both are supported, in part, with funding from National Institute of Health (NIH)-National Cancer Institute Cancer Center Support Grant P30 CA016059.

# References

1. Santini V, Kantarjian HM, Issa JP. Changes in DNA methylation in neoplasia: pathophysiology and therapeutic implications. Ann Intern Med. 2001 Apr;134(7):573–86.
2. Diaz-Montero CM, Salem ML, Nishimura MI, Garrett-Mayer E, Cole DJ, Montero AJ. Increased circulating myeloid-derived suppressor cells correlate with clinical cancer stage, metastatic tumor burden, and doxorubicin-cyclophosphamide chemotherapy. Cancer Immunol Immunother. 2009 Jan;58(1):49–59.
3. Gonda K, Shibata M, Ohtake T, Matsumoto Y, Tachibana K, Abe N, et al. Myeloid-derived suppressor cells are increased and correlated with type 2 immune responses, malnutrition, inflammation, and poor prognosis in patients with breast cancer. Oncol Lett. 2017;14(2):1766–74.
4. Wang L, Chang EWY, Wong SC, Ong S-M, Chong DQY, Ling KL. Increased Myeloid-Derived Suppressor Cells in Gastric Cancer Correlate with Cancer Stage and Plasma S100A8/A9 Proinflammatory Proteins. J Immunol. 2013;190(2):794–804.
5. Sio A, Chehal MK, Tsai K, Fan X, Roberts ME, Nelson BH, et al. Dysregulated hematopoiesiscausedbymammary Cancer is associated with epigenetic changes and Hox gene expression in hematopoietic cells. Cancer Res. 2013;73(19):5892–904.
6. Choi HS, Ha SY, Kim H-M, Ahn SM, Kang M-S, Kim K-M, et al. The prognostic effects of tumor infiltrating regulatory T cells and myeloid derived suppressor cells assessed by multicolor flow cytometry in gastric cancer patients. Oncotarget. 2016 Feb;7(7):7940–51.

7. Ugel S, Peranzoni E, Desantis G, Chioda M, Walter S, Weinschenk T, et al. Immune Tolerance to Tumor Antigens Occurs in a Specialized Environment of the Spleen. Cell Rep. 2012 Sep 27;2(3):628–39.
8. Alizadeh D, Trad M, Hanke NT, Larmonier CB, Janikashvili N, Bonnotte B, et al. Doxorubicin eliminates myeloid-derived suppressor cells and enhances the efficacy of adoptive T-cell transfer in breast cancer. Cancer Res. 2014 Jan;74(1):104–18.
9. Ostrand-Rosenberg S, Fenselau C. Myeloid-Derived Suppressor Cells: Immune-Suppressive Cells That Impair Antitumor Immunity and Are Sculpted by Their Environment. J Immunol. 2018;200:422–31.
10. Terracina KP, Graham LJ, Payne KK, Manjili MH, Baek A, Damle SR, et al. DNA methyltransferase inhibition increases efficacy of adoptive cellular immunotherapy of murine breast cancer. Cancer Immunol Immunother. 2016 Sep;65(9):1061–73.
11. Talmadge JE, Gabrilovich DI, Immunology TT. History of myeloid derived suppressor cells (MDSCs) in the macro- and micro-environment of tumour-bearing hosts. Nat Rev Cancer. 2013;13(10):739–52.
12. duPre' SA, Hunter KW. Murine mammary carcinoma 4T1 induces a leukemoid reaction with splenomegaly: Association with tumor-derived growth factors. Exp Mol Pathol. 2007 Feb;82(1):12–24.
13. Bronte V, Wang M, Overwijk WW, Surman DR, Pericle F, Rosenberg SA, et al. Apoptotic death of CD8+ T lymphocytes after immunization: induction of a suppressive population of Mac–1+/Gr–1+ cells. J Immunol. NIH Public Access; 1998 Nov;161(10):5313–20.
14. Kusmartsev SA, Li Y, Chen SH. Gr–1+ myeloid cells derived from tumor-bearing mice inhibit primary T cell activation induced through CD3/CD28 costimulation. J Immunol. 2000 Jul;165(2):779–85.
15. Raber PL, Thevenot P, Sierra R, Wyczechowska D, Halle D, Ramirez ME, et al. Subpopulations of myeloid-derived suppressor cells impair T cell responses through independent nitric oxide-related pathways. Int J Cancer. 2014;134(12):2853–64.
16. Kusmartsev S, Gabrilovich DI. Role Of Immature Myeloid Cells in Mechanisms of Immune Evasion In Cancer. Cancer Immunol Immunother. 2006 Mar;55(3):237–45.
17. Bronte V, Apolloni E, Cabrelle A, Ronca R, Serafini P, Zamboni P, et al. Identification of a CD11b(+)/Gr–1(+)/CD31(+) myeloid progenitor capable of activating or suppressing CD8(+) T cells. Blood. 2000 Dec 1;96(12):3838–46.
18. Kusmartsev S, Gabrilovich DI. Inhibition of myeloid cell differentiation in cancer : the role of reactive oxygen species. Cancer. 2003;74(August).
19. Gabrilovich DI, Velders MP, Sotomayor EM, Kast WM. Mechanism of immune dysfunction in cancer mediated by immature Gr–1+ myeloid cells. J Immunol. 2001 May;166(9):5398–406.
20. Zhou J, Yao Y, Shen Q, Li G, Hu L, Zhang X. Demethylating agent decitabine disrupts tumor-induced immune tolerance by depleting myeloid-derived suppressor cells. J Cancer Res Clin Oncol. 2017 Aug;143(8):1371–80.
21. Liu Y, Van Ginderachter JA, Brys L, De Baetselier P, Raes G, Geldhof AB. Nitric oxide-independent CTL suppression during tumor progression: association with arginase-producing (M2) myeloid cells. J Immunol. 2003 May;170(10):5064–74.

22. Chandrasekaran S, King M. Microenvironment of Tumor-Draining Lymph Nodes: Opportunities for Liposome-Based Targeted Therapy. Int J Mol Sci. 2014 Nov;15(11):20209–39.
23. Duan F, Simeone S, Wu R, Grady J, Mandoiu I, Srivastava PK. Area under the curve as a tool to measure kinetics of tumor growth in experimental animals. J Immunol Methods. 2012 Aug;382(1–2):224–8.
24. Triozzi PL, Aldrich W, Achberger S, Ponnazhagan S, Alcazar O, Saunthararajah Y. Differential effects of low-dose decitabine on immune effector and suppressor responses in melanoma-bearing mice. Cancer Immunol Immunother. 2012 Sep;61(9):1441–50.
25. Lucarini V, Buccione C, Ziccheddu G, Peschiaroli F, Sestili P, Puglisi R, et al. Combining Type I Interferons and 5-Aza–2'-Deoxycitidine to Improve Anti-Tumor Response against Melanoma. J Invest Dermatol. 2017 Jan;137(1):159–69.
26. Le HK, Graham L, Cha E, Morales JK, Manjili MH, Bear HD. Gemcitabine directly inhibits myeloid derived suppressor cells in BALB/c mice bearing 4T1 mammary carcinoma and augments expansion of T cells from tumor-bearing mice. Int Immunopharmacol. 2009 Jul;9(7–8):900–9.
27. Suzuki E, Kapoor V, Jassar AS, Kaiser LR, Albelda SM. Gemcitabine Selectively Eliminates Splenic Gr–1+/CD11b+ Myeloid Suppressor Cells in Tumor-Bearing Animals and Enhances Antitumor Immune Activity. Clin Cancer Res. 2005 Sep;11(18):6713–21.
28. Kodumudi KN, Woan K, Gilvary DL, Sahakian E, Wei S, Djeu JY. A Novel Chemoimmunomodulating Property of Docetaxel: Suppression of Myeloid-Derived Suppressor Cells in Tumor Bearers. Clin Cancer Res. 2010 Sep;16(18):4583–94.
29. Liu Y, Wei G, Cheng WA, Dong Z, Sun H, Lee VY, et al. Targeting myeloid-derived suppressor cells for cancer immunotherapy. Cancer Immunol Immunother. 2018 Aug;67(8):1181–95.
30. Albeituni SH, Ding C, Liu M, Hu X, Luo F, Kloecker G, et al. Yeast-Derived Particulate β-Glucan Treatment Subverts the Suppression of Myeloid-Derived Suppressor Cells (MDSC) by Inducing Polymorphonuclear MDSC Apoptosis and Monocytic MDSC Differentiation to APC in Cancer. J Immunol. 2016 Mar 1;196(5):2167–80.
31. Vila-Leahey A, Oldford SA, Marignani PA, Wang J, Haidl ID, Marshall JS. Ranitidine modifies myeloid cell populations and inhibits breast tumor development and spread in mice. Oncoimmunology. 2016 Jul 2;5(7):e1151591.
32. Saleem SJ, Martin RK, Morales JK, Sturgill JL, Gibb DR, Graham L, et al. Cutting edge: mast cells critically augment myeloid-derived suppressor cell activity. J Immunol. 2012 Jul 15;189(2):511–5.
33. Unkeless JC. Characterization of a monoclonal antibody directed against mouse macrophage and lymphocyte Fc receptors. J Exp Med. Rockefeller University Press; 1979 Sep 19;150(3):580–96.

# Figures

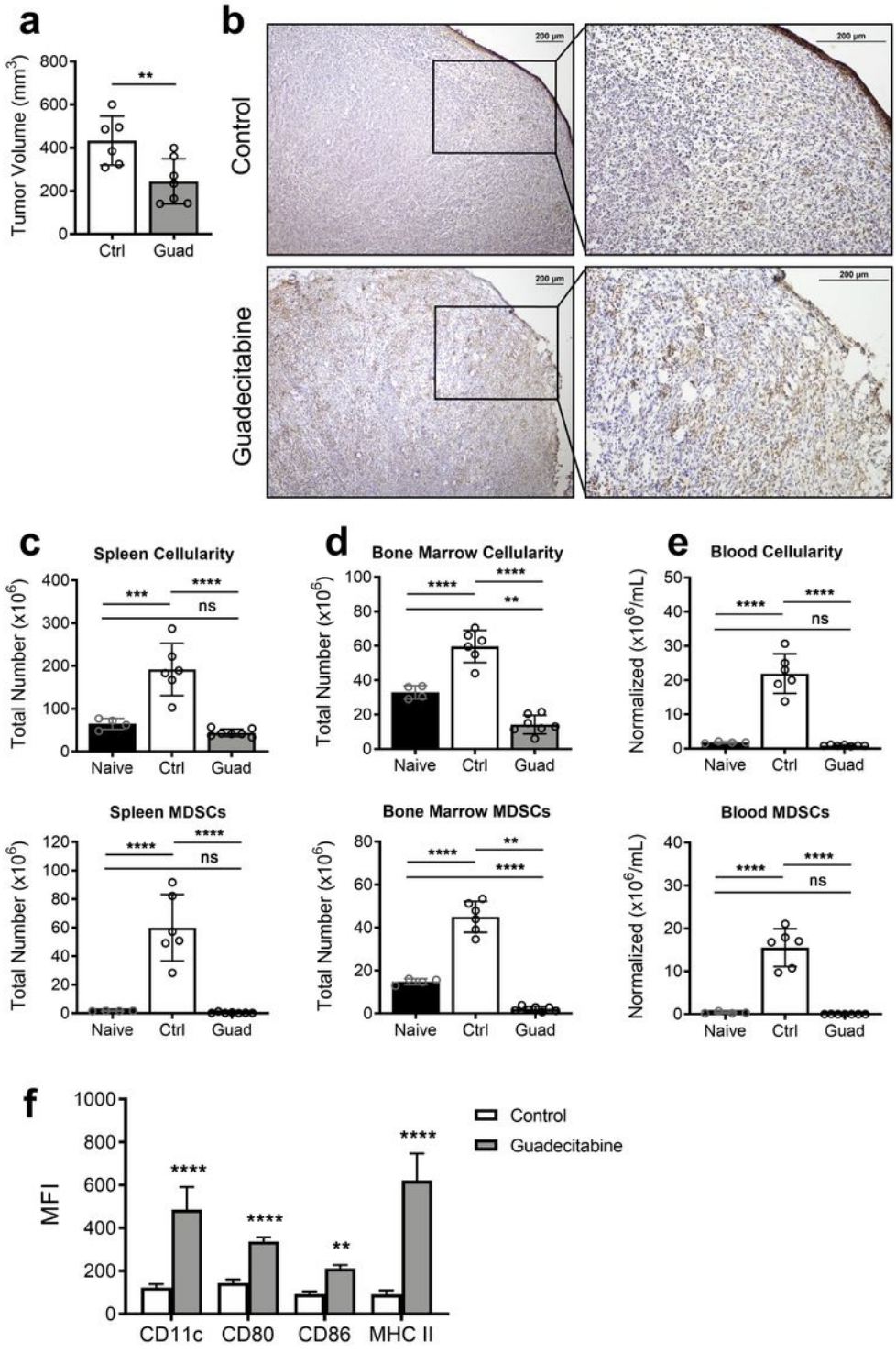


## Figure 1

Guadecitabine treatment results in smaller tumors and a reduction in myeloid cells. 4T1 tumor-bearing mice were treated with guadecitabine on days 10-13. a Final volume of excised tumors on day 16. b Representative images of frozen tumor sections stained with TUNEL to detect apoptotic cells. Total cellularity (top) and number of MDSCs (bottom) from c spleen, d bone marrow, and e blood. f Surface expression of APC markers on splenic MDSCs. Significance determined using student's unpaired T test

(a), ANOVA with Tukey's (c-e) or Sidak's (f) multiple comparison tests. Error bars represent SD. ns= not significant; **:p value<0.0021; ***:p value<0.0002; ****:p value<0.00001.

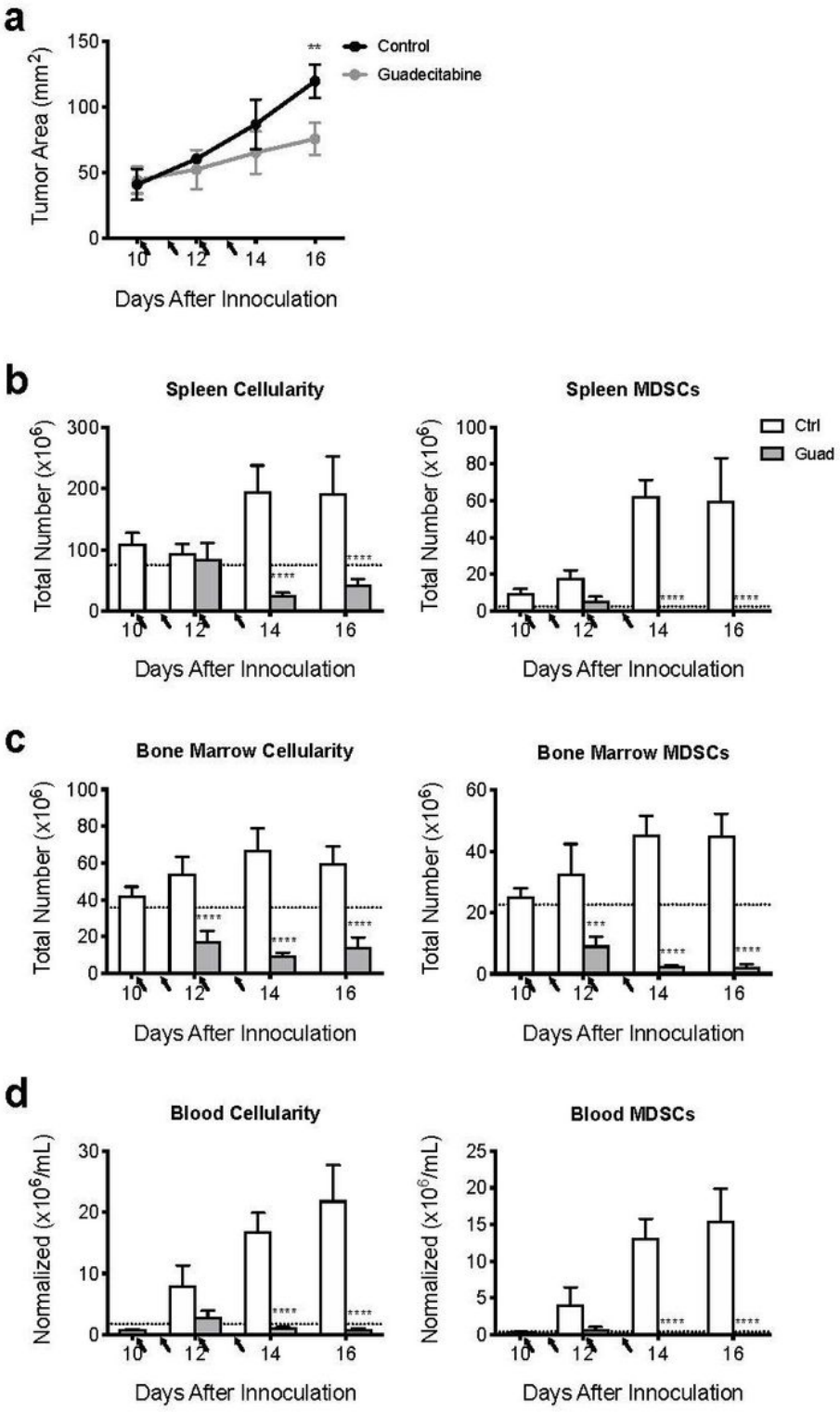


## Figure 2

Guadecitabine slows tumor growth and immediately reverses the rapidly expanding myeloid population. a Timecourse experiment showing 4T1 tumor growth in WT balb/c mice. Total cellularity and number of MDSCs from b spleen, c bone marrow, and d blood. Arrows indicate guadecitabine treatments; dotted line

indicates naïve levels. Significance determined using ANOVA with Sidak's multiple comparison tests. Error bars represent SD. ns= not significant, *:p value<0.0332; **:p value<0.0021; ***:p value<0.0002; ****:p value<0.00001.

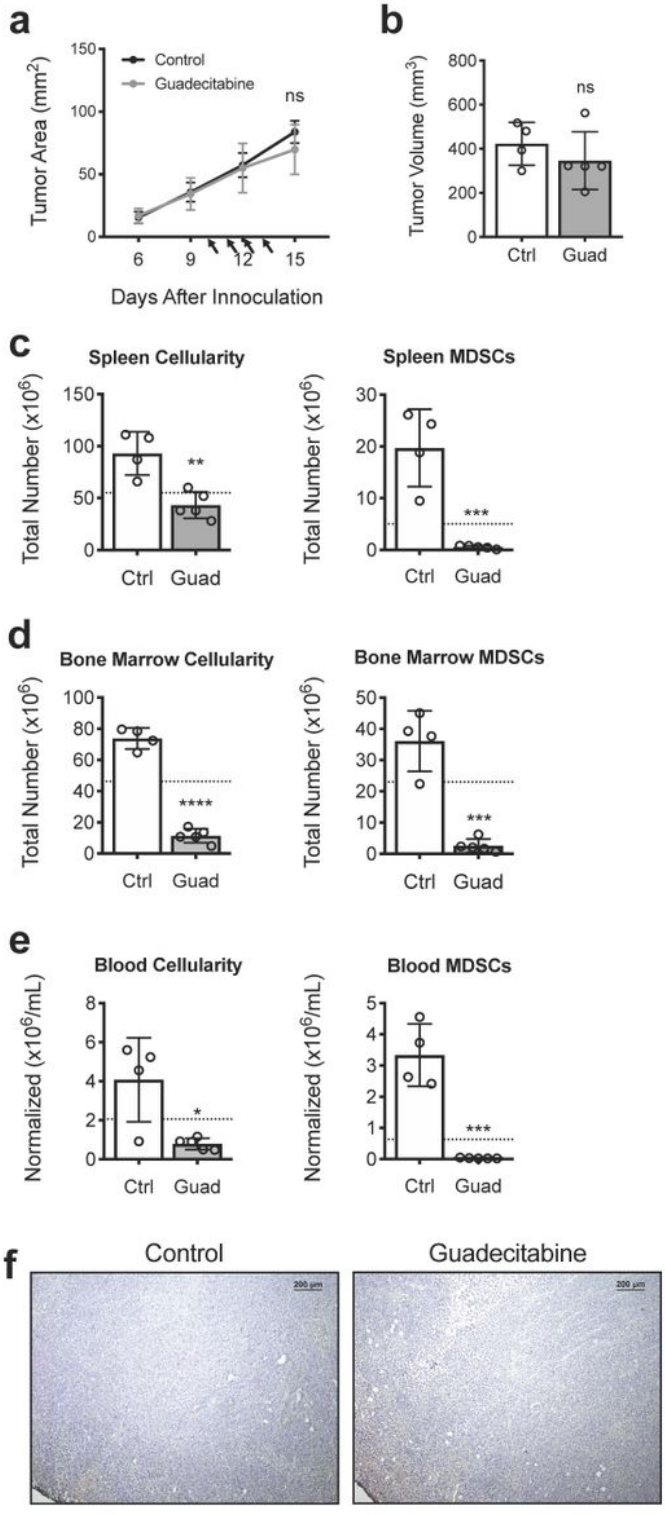


## Figure 3

Tumor growth in T cell-deficient mice is not affected by guadecitabine. 4T1 tumor challenge in athymic mice, showing a tumor growth curve and b final excised tumor volume at day 16. Total cellularity and

number of MDSCs from c spleen, d bone marrow, and e blood. f Representative images of day 16 frozen tumor sections stained with TUNEL. Dotted line indicates naïve levels. Significance determined by unpaired student's T-test. Error bars represent SD. ns= not significant; *:p value<0.0332; **:p value<0.0021; ***:p value<0.0002; ****:p value<0.00001.

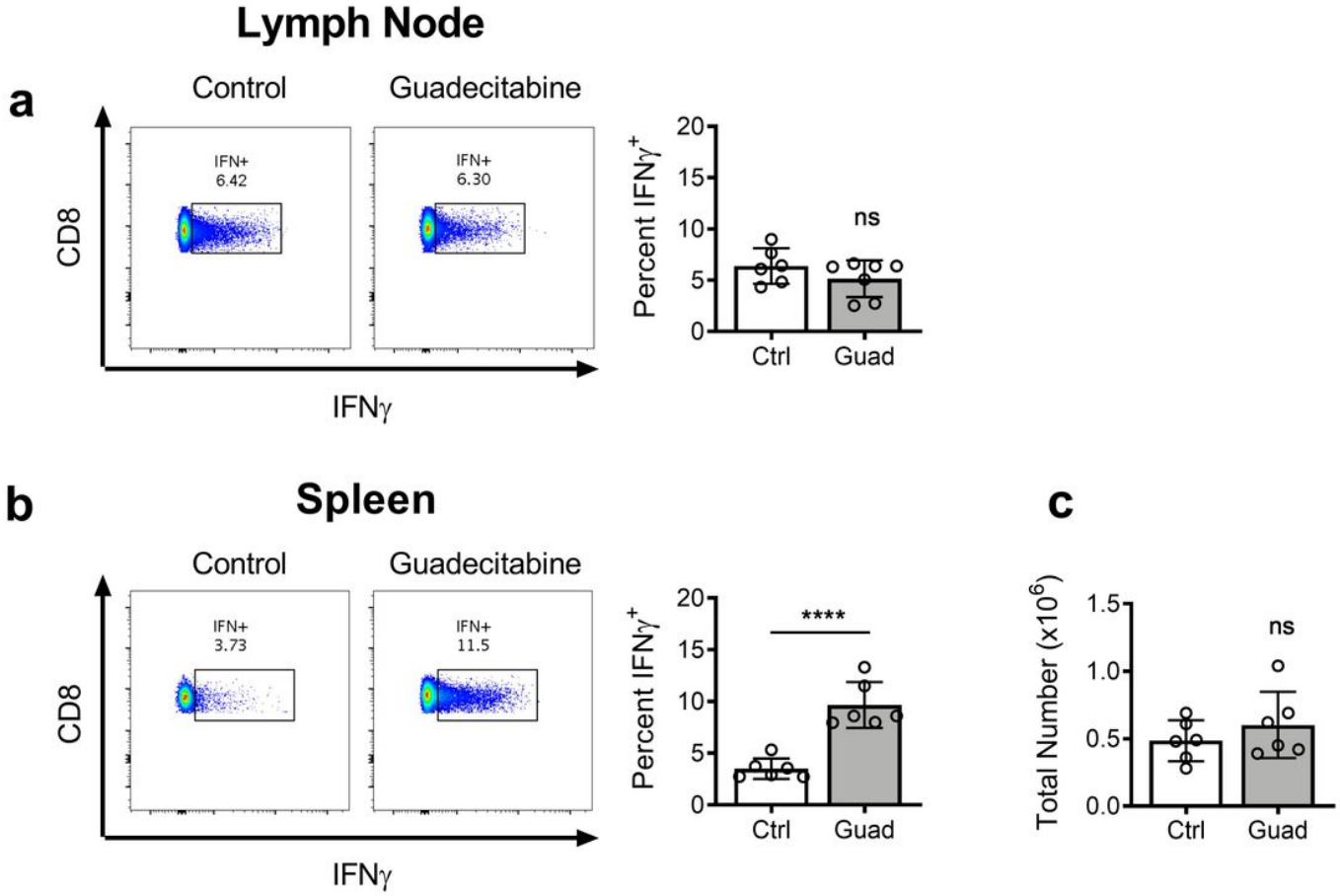


## Figure 4

Guadecitabine boosts the CD8+ T cell anti-tumor response in the spleen. IFN□ production by a lymphocytes and b splenocytes from tumor-bearing mice following ex vivo restimulation for 3 hours with ionomycin and PMA. c Total number of IFN□-producing CD8+ splenocytes. Significance determined by unpaired student's T-test. Error bars represent SD. ns=not significant; ****:p value<0.00001.

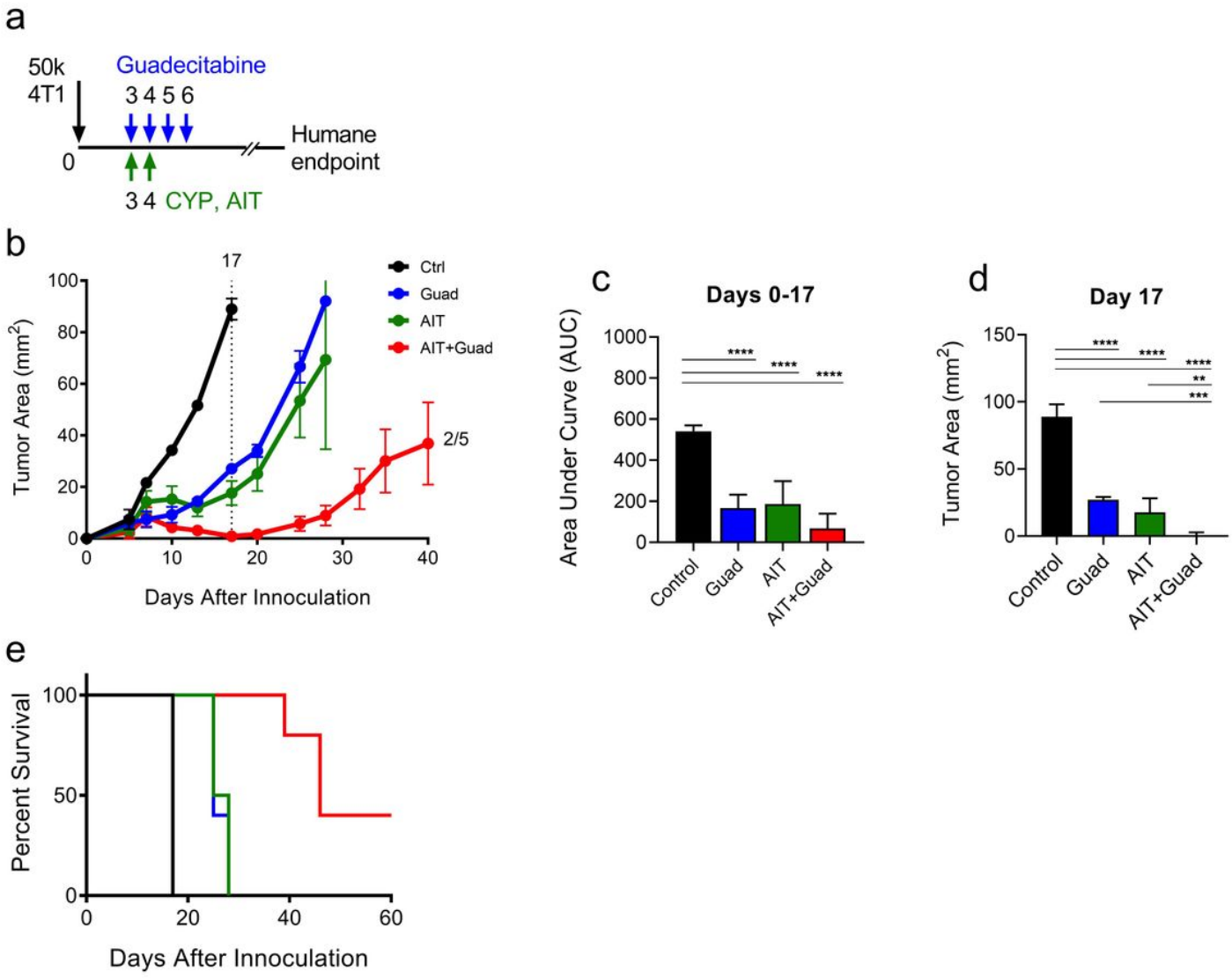


## Figure 5

Combination therapy of guadecitabine and AIT slows tumor growth and improves overall survival. a 4T1 tumor-bearing mice were treated with guadecitabine on days 3-6, then received CYP and 25 million antigen-experienced lymphocytes on days 3,4. b Tumor progression was measured until humane endpoints were reached; dotted line indicates day statistical significance was determined by c area under the curve or d tumor area. e Survival curves depicting overall survival in each treatment group. Significance determined using ANOVA with Tukey's multiple comparison test Error bars represent SEM. *:p value<0.0332; **:p value<0.0021; ***:p value<0.0002; ****:p value<0.00001.

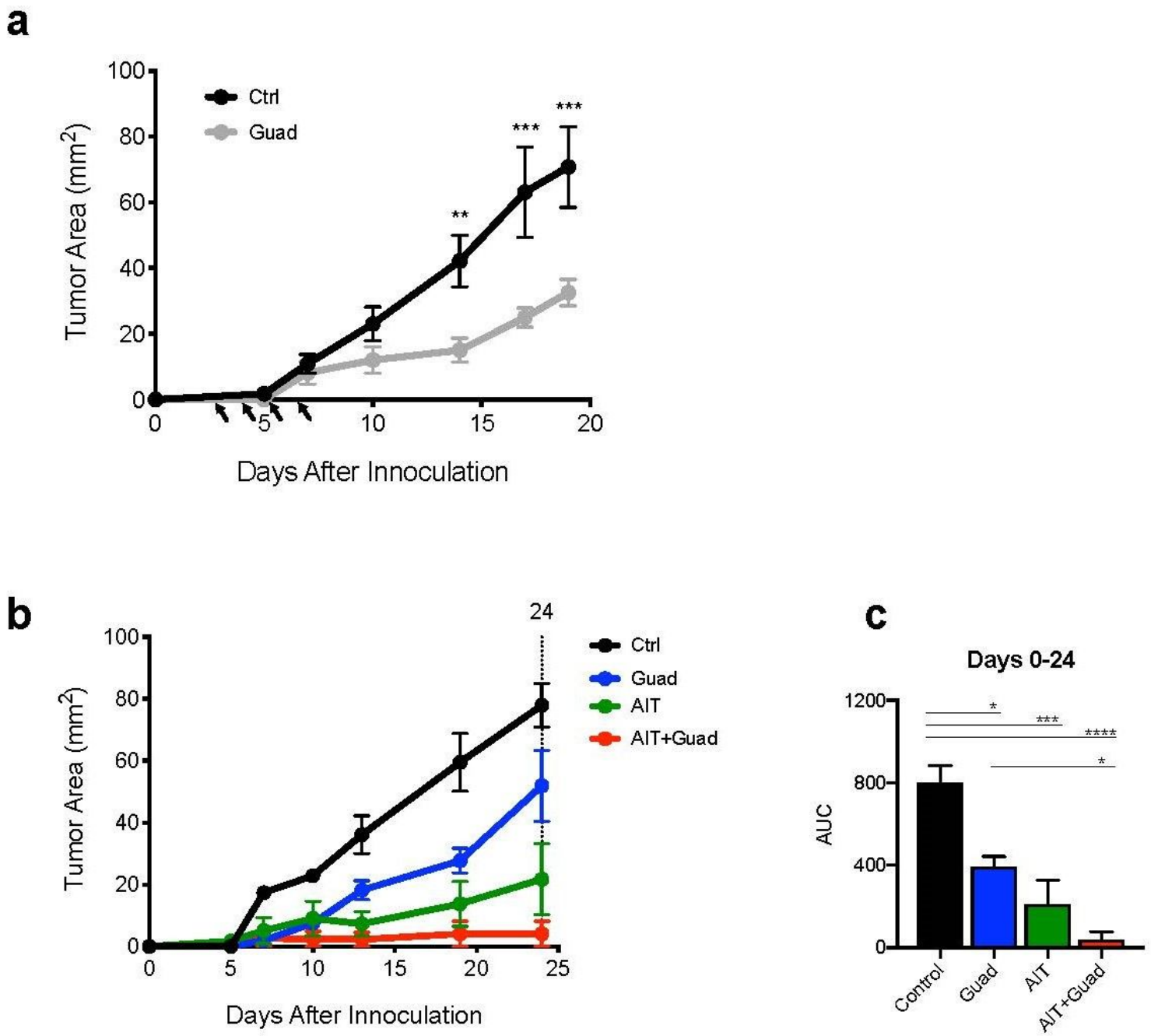


**Figure 6**

Guadecitabine similarly reduces E0771 tumor size and improves effectiveness of AIT. E0771 tumor-bearing mice were treated with guadecitabine on days 3-6. a Time-course experiment showing E0771 tumor growth in WT C57Bl/6 mice. b E0771 tumor progression following AIT treatment as in Fig 5. c AUC quantification of tumorgrowth following combination therapy. Significance determined using ANOVA with Sidak's (a) or Tukey's (c) multiple comparison test. Error bars represent SEM. *:p value<0.0332; **:p value<0.0021; ***:p value<0.0002; ****:p value<0.00001.

# Supplementary Files

This is a list of supplementary files associated with this preprint. Click to download.

- SuppFinalmerged.pdf
- NC3RsARRIVEGuidelinesChecklistrkmHDB9232019.pdf